

# Polymerization, Stimuli-induced Depolymerization, and Precipitation-driven Macrocyclization in a Nitroaldol Reaction System

Yunchuan Qi,<sup>1</sup> Olof Ramström\*<sup>1,2</sup>

<sup>1</sup>*Department of Chemistry, University of Massachusetts Lowell, One University Ave., Lowell, MA 01854, USA;*  
*Email: olof\_ramstrom@uml.edu;* <sup>2</sup>*Department of Chemistry and Biomedical Sciences, Linnaeus University,*  
*SE-39182 Kalmar, Sweden*

## Abstract

Dynamic covalent polymers of different topology have been synthesized from an aromatic dialdehyde and  $\alpha,\omega$ -dinitroalkanes via the nitroaldol reaction. All dinitroalkanes yielded dynamers with the dialdehyde, where the length of the dinitroalkane chain played a vital role in determining the structure of the final products. For longer dinitroalkanes, linear dynamers were produced, where the degree of polymerization reached a plateau at higher feed concentrations. In the reactions involving 1,4-dinitrobutane and 1,5-dinitropentane, specific macrocycles were formed through depolymerization of the linear chains, further driven by precipitation. At lower temperature, the same systemic self-sorting effect was also observed for the 1,6-dinitrohexane-based dynamers. Moreover, the dynamers showed a clear adaptive behavior, displaying depolymerization and rearrangement of the dynamer chains in response to alternative building blocks as external stimuli.

## Introduction

Complex entities constructed by reversible covalent bonds have demonstrated fascinating dynamic behaviors and rich functionalities.<sup>1–17</sup> For example, main-chain dynamic covalent polymers (dynamers), in which the repeating units are connected by dynamic covalent bonds, show great potential in the development of novel functional materials for a wide range of applications. For example, dynamers show intriguing malleability, recyclability, self-healing, stimuli-responsiveness, shape-memory and shear-thinning effects, as well as tunable mechanical and optical properties.<sup>2,4,18–23</sup> These materials are characterized by their adaptive properties, able to predictably respond to various stimuli, and can give rise to emergent properties.<sup>4,11,24–27</sup>

A variety of dynamic covalent reactions have been applied to dynamer formation, such as imine formation (incl. hydrazones, oximes, etc.),<sup>28–32</sup> reversible cycloadditions (incl. olefin metathesis),<sup>1,33–35</sup> acetals,<sup>36</sup> transesterifications (incl. boronates),<sup>37–43</sup> and reactions involving disulfides.<sup>12,44</sup> Among these, reactions that can generate carbon-carbon bonds are of special interest since transformations are responsible for building up the carbon backbone of organic molecules and materials.<sup>45</sup> Hence, employing reversible C–C bonds in molecules can potentially increase the dynamic performance of the whole entity since even the molecular skeleton is dynamic.<sup>3</sup>

Due to its efficiency in generating new C–C bonds, the nitroaldol (Henry) reaction has been widely applied in organic synthesis since it was first discovered in 1895.<sup>46–48</sup> The reaction is robust, stereogenic, self-contained, and can be carried out under mild conditions. Studies have also shown its excellent performance in dynamic and systems chemistry,<sup>14,45,49–51</sup> and in the synthesis of dynamers under aqueous conditions.<sup>3</sup> However, the scope and application of the nitroaldol reaction in dynamer synthesis still require a much-needed expansion.

In our previous study,<sup>3</sup> we exploited nitromethane as a bifunctional nitrocompound in dynamer synthesis, since it enables multiple nitroaldol reaction steps at the same carbon center (**Figure 1a**).<sup>52</sup> The degree of polymerization of these dynamers was limited (ca. 17), likely due to the steric hindrance and lower reactivity of the remaining  $\alpha$ -protons after the first nitroaldol reaction. To circumvent this limitation, we applied  $\alpha,\omega$ -dinitroalkanes as building blocks in the present study, able to provide relatively equal reactivities at either end of the chains (**Figure 1b**).

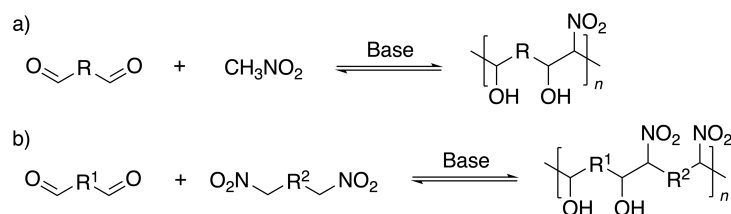


**Figure 1:** Polymerization via the nitroaldol reaction; a) previous report;<sup>3</sup> b) this study.

An important challenge with dynamers is the generation and control of different oligomeric and polymeric topologies, as well as their relative stimuli-responsive properties. Since dynamer systems rely on multiple, sequential or parallel dynamic covalent reactions, the systems may undergo complex topology changes over time, potentially leading to self-sorting of specific structures. Furthermore, such processes may lead to emergent property changes, and a detailed understanding of these processes is, therefore, of significant value for future applications.

Herein, we report the generation and evaluation of complex nitroaldol systems involving a dialdehyde and a series of  $\alpha,\omega$ -dinitroalkanes. In all cases, dynamers were formed, and the interplay between different topologies were studied. The dynamerization process was evaluated with respect to dinitroalkane structure, catalyst loading, and feed concentration, and kinetic studies were performed. Intriguingly, specific macrocyclization was observed in several systems, occurring in competition with the formation of linear dynamers. This gave rise to polymerization/depolymerization processes, in several cases undergoing further self-sorting through phase changes (**Figure 2**). Moreover, the stimuli-responsive behavior of the dynamers were explored.

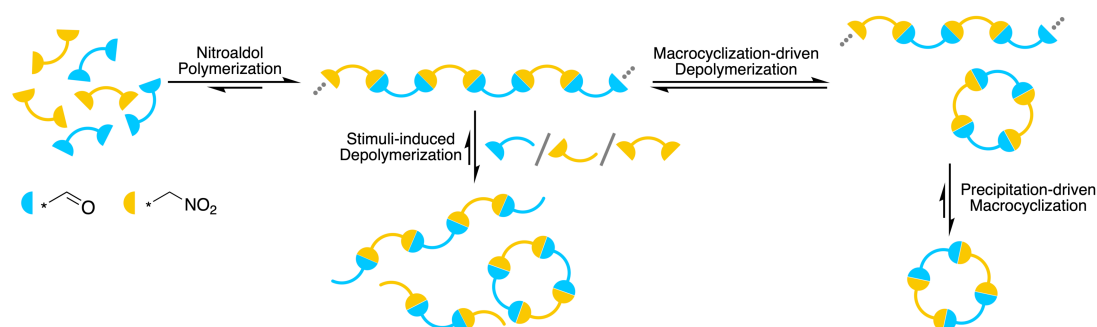


**Figure 2:** Nitroaldol dynamer formation, topology changes, self-sorting, and stimuli-responsiveness.

## Results and Discussion

Based on our previous report,<sup>3</sup> 2,6-pyridinedicarboxaldehyde (**1**) was chosen as the dialdehyde building block because of its high reactivity in the nitroaldol reaction. In complement to this, eight  $\alpha,\omega$ -dinitroalkanes (**2**), including 1,3-dinitropropane (**2a**), 1,4-dinitrobutane (**2b**), 1,5-dinitropentane (**2c**), 1,6-dinitrohexane (**2d**), 1,7-dinitroheptane (**2e**), 1,8-dinitrooctane (**2f**),

1,9-dinitrononane (**2g**), and 1,10-dinitrodecane (**2h**), were selected as dinitroalkane building blocks (**Figure 3**). Triethylamine ( $\text{Et}_3\text{N}$ ) was used as base throughout, and all reactions were carried out in acetonitrile due to the high solubility of the starting materials in this solvent. Under these conditions, dual entryptone equilibration analysis indicated that the proposed nitroaldol polymerization operated under thermodynamic control (cf. Supporting Information, Figure S21).

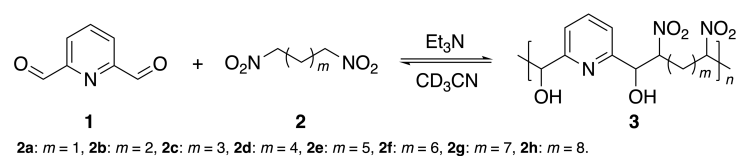


**Figure 3:** Proposed nitroaldol polymerization system.

Polymers were generated from all systems within 48 h, as demonstrated by the broad signals in the  $^1\text{H}$ -NMR spectra (**Figure 4**). Interestingly, white precipitates were formed in the systems containing the shorter dinitroalkanes **2b** and **2c**, whereas the solutions of the reactions with the other dinitroalkanes remained clear. Nevertheless, the formation of dynamers **3b** and **3c** resulted in spectra with typical nitroaldol characteristics, showing new nitroalcohol signals at 5.7–4.5 ppm. Dynamers **3d–3h**, having longer alkyl linkers, all produced relatively similar spectra apart from the hydroxyl protons shifts. High conversions of the starting materials were observed in all cases, and the resonances of the aldehyde protons (10.1 ppm) and the  $\alpha$ -protons of the nitroalkane (4.57–4.38 ppm) nearly disappeared.

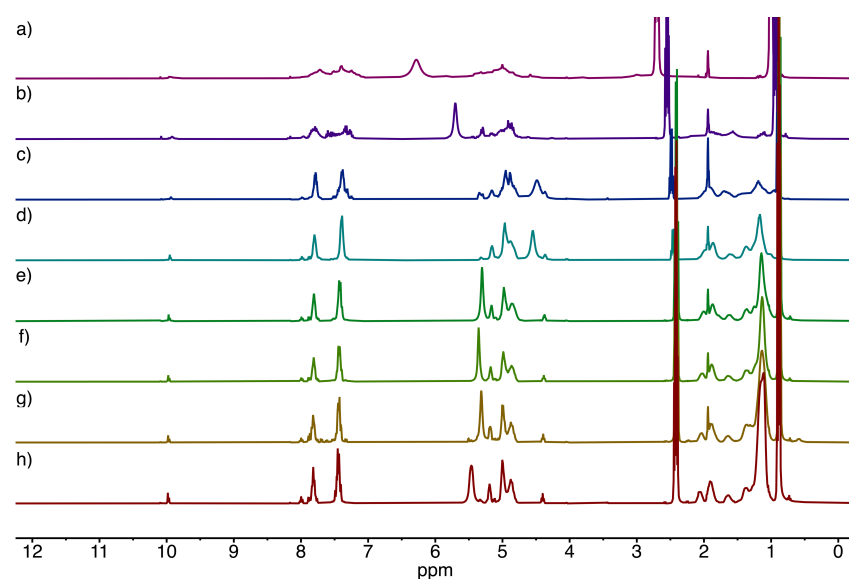


**Figure 4:**  $^1\text{H}$  NMR spectra of a) **3a**; b) **3b**; c) **3c**; d) **3d**; e) **3e**; f) **3f**; g) **3g**; h) **3h** in solution (1.5 M feed concentration, 10 mol%  $\text{Et}_3\text{N}$ ; 400 MHz,  $\text{CD}_3\text{CN}$ ).

The products of the polymerization process were analyzed by diffusion-ordered NMR spectroscopy (DOSY NMR) and gel permeation chromatography (GPC). The DOSY experiments revealed the formation of species with diffusion coefficients in the range of  $(0.26\text{--}1.10)\times 10^{-10}$   $\text{cm}^2/\text{s}$  in all eight dynamer systems, indicating the formation of oligomers or polymers (**Table 1**, Figure S22–S29).<sup>53</sup>

Further information of the molecular weights and the weight distributions of the dynamers were provided by GPC (**Table 1**) from which clear trends could be discerned. In general,

longer alkyl chains in the starting dinitroalkanes gave rise to higher molecular weights of the produced polymers. The degree of polymerization (DP) increased from dynamer **3a** to dynamer **3d** and reached a plateau at around 34 from dynamer **3d** to dynamer **3h**. The lower degree of polymerization for the shorter dinitroalkanes is likely an effect of steric hindrance (dynamer **3a**), possibly coupled with the precipitation of insoluble products (dynamers **3b–3c**). On the other hand, the comparable structure and reactivity of the longer dinitroalkanes (**2d–2h**), resulted in the generation of dynamers with very similar degrees of polymerization. Given the high solubility of the products, this is a reflection of the concentration-dependent polymer growth and the dynamics of the polymerization reaction. At a concentration threshold of around 45 mM of the starting materials, the rates of polymerization and depolymerization were thus balanced. Moreover, dynamers **3a–3c** showed relatively low polydispersity indices ( $\mathcal{D}$ ), indicating the formation of shorter, more homogeneous oligomers; whereas dynamers **3d–3h** all had a wider molecular weight distribution ( $\mathcal{D} = 1.7$ ).

**Table 1:** DOSY NMR and GPC data of dynamers **3a–3h** (1.5 M feed concentration).

Dynamer	$D$ (cm <sup>2</sup> /s)	$M_n$ (g/mol)	$M_w$ (g/mol)	$M_z$ (g/mol)	$\mathcal{D}$	DP
<b>3a</b>	$1.10 \times 10^{-10}$	2700	3100	3600	1.1	10
<b>3b</b>	$1.69 \times 10^{-10}$	2700	2900	3200	1.1	9
<b>3c</b>	$2.30 \times 10^{-10}$	6300	8700	12400	1.4	21
<b>3d</b>	$3.46 \times 10^{-11}$	10400	17500	28000	1.7	33
<b>3e</b>	$8.29 \times 10^{-11}$	10500	18100	30200	1.7	32
<b>3f</b>	$5.40 \times 10^{-11}$	11800	20400	33300	1.7	35
<b>3g</b>	$4.61 \times 10^{-11}$	12100	20700	33100	1.7	34
<b>3h</b>	$2.60 \times 10^{-11}$	12000	20300	32500	1.7	34

$D$ : diffusion coefficient;  $\mathcal{D}$ : polydispersity index; DP: degree of polymerization

Further NMR and MS analysis (Figure S38–S49) indicated that the precipitates in the systems involving dialdehyde **1** and dinitroalkane **2b**, as well as dialdehyde **1** with dinitroalkane **2c**, were composed of cyclic molecules, coined as *lowellanes*, instead of polymers (Figure 5a). Macrocyclization in nitroaldol-based systems is in this context of high interest, leading to cyclic, flexible carbon chains involving multiple stereocenters, in complement to previously observed cyclization in molybdenum-catalyzed alkyne metathesis and imine exchange.<sup>30,54,55</sup>

To investigate the macrocyclization process in our system, dialdehyde **1** and dinitroalkane **2b** were dissolved in acetonitrile at a feed concentration of 0.5 M. After adding 10 mol% of Et<sub>3</sub>N, aliquots of the solution were withdrawn periodically and analyzed by GPC. The resulting GPC-profile revealed that the reaction products were mainly short oligomers ( $M_n = 3700$ , DP = 6) in the early stage of the reaction. However, at longer reaction times, the oligomer concentration decreased while the amount of lowellane **7**, composed of two of each building block (DP corresponding to 2), increased (Figure 5b, Figure S50–S59). Thus, a depolymerization process promoted by macrocyclization took place over time, further driven by precipitation of the formed macrocycle. In general, macrocyclization coupled to linear polymerization indicates a ring-chain polymerization process, observed with both supramolecular and covalent polymers,<sup>56</sup> where macrocyclization is favored under high dilution conditions, and linear polymerization takes place at higher concentrations. However, the macrocyclization behavior in the present system suggests a special case in agreement with a ring-closing depolymerization process.<sup>57</sup> Thus, in this case, the rate of depolymerization is significantly lower than the rate of macrocyclization, thereby generating transient linear polymers that gradually degrade over time in response to macrocycle formation. Moreover, the

dynamic system constituted a self-sorting process, amplified by solubility constraints, and, although multiple macrocyclic species in principle could be formed, only lowellane **7** was formed.

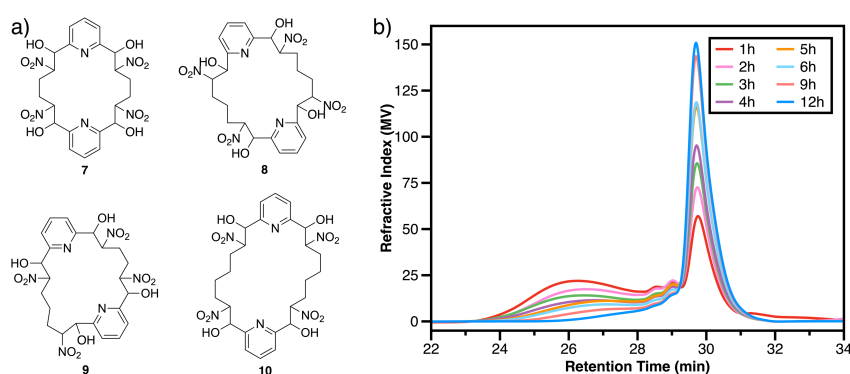


**Figure 5:** a) Structures of lowellane macrocycles **7–10**; b) GPC profile of the reaction between compounds **1** and **2b** from 1 h to 12 h.

At room temperature, the precipitation-driven process was only observed with dinitroalkanes **2b** and **2c**. However, when the temperature was lowered to 8 °C, the macrocycle self-sorting process was also observed with dinitroalkane **2d**. The process was in this case slower, and lowellane **10**, composed of two dialdehyde and two dinitrohexane building blocks, only precipitated from the polymerization solution after several weeks.

Furthermore, the reaction of dialdehyde **1** with both dinitroalkanes **2b** and **2c** in the same mixture was carried out in acetonitrile. The reaction yielded a mixture of macrocycles, including lowellanes **7** and **8**, as well as hybrid lowellane **9**, all composed of two repeating units (Figure 5a). This further demonstrates the dynamic nature of the nitroaldol polymerization system. Unfortunately, the separation of the macrocyclic species from the crude product proved challenging, so compound **9** could only be observed by ESI-MS (Figure S48).

To better understand the polymerization systems in which macrocyclization did not occur, a kinetic study was carried out using the reaction between dialdehyde **1** and dinitroalkane **2d** at room temperature in CD<sub>3</sub>CN. The <sup>1</sup>H-NMR spectra show that the reaction proceeded rapidly during the first hour after Et<sub>3</sub>N was added (Figure 6a), and then significantly slowed down (Figure S60). Using 1,4-dioxane as the internal standard, the concentration change and conversion of compound **1** over time was calculated. The results reveal that the consumption of dialdehyde **1** matches first-order kinetics during the first hour, with a rate coefficient (*k*) of 1.27×10<sup>-3</sup>/s (Figure 6b). Under these conditions, the relation between the number-average molecular weight (*M<sub>n</sub>*) and the conversion of dialdehyde **1** from the GPC and <sup>1</sup>H-NMR data approximately fits a step-growth polymerization model (Figure 6c, Figure S61–S70).<sup>58</sup>

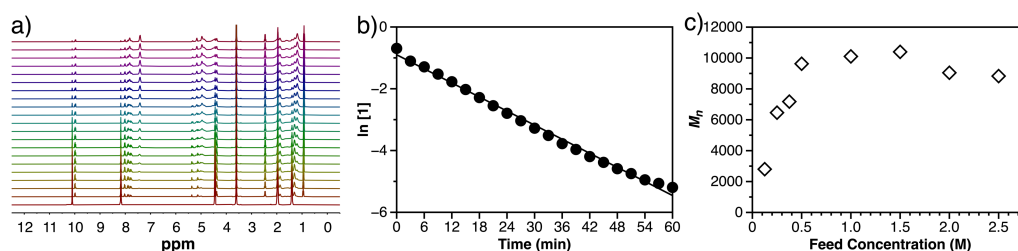


**Figure 6:** a)  $^1\text{H-NMR}$  spectra of reaction between compounds **1** and **2d** in  $\text{CD}_3\text{CN}$  at 0–60 min. (3 min interval; 0.5 M; 10 mol%  $\text{Et}_3\text{N}$ ; rt; 1,4-dioxane as internal standard ( $\delta$  3.57 ppm); 400 MHz); b) Consumption of dialdehyde **1** following first-order kinetics; c)  $M_n$  as function of conversion of compound **1**.

The effect of the molar fraction of  $\text{Et}_3\text{N}$  (5–25 mol% of compound **1**) on the reaction kinetics was also investigated by  $^1\text{H-NMR}$ . The reaction was found to be approximately first order in  $\text{Et}_3\text{N}$ , and the reaction rate constant increased with the amount of  $\text{Et}_3\text{N}$  within the first hour (Figure 7a,  $\Delta$ ). After 12 h, when all reactions had reached equilibria, the final products showed almost identical  $^1\text{H-NMR}$  spectra despite the difference in base percentage (Figure S76). On the other hand, the GPC results reveal clearer differences between the polymers (Table S4). The  $M_n$  of the polymer prepared using 5 mol% of  $\text{Et}_3\text{N}$  was slightly lower than those made with higher ratios of base, although the difference was not significant in the range of 10–25 mol% (Figure 7a,  $\blacksquare$ ).

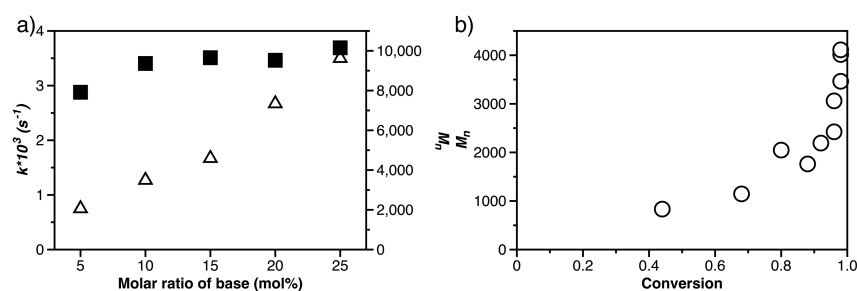


**Figure 7:** a) Rate constants of **1** in its reaction with **2d** with different amount of base ( $\Delta$ );  $M_n$  of polymers with different amount of base ( $\blacksquare$ ). (0.5 M feed concentration); b) Effect of feed concentration on  $M_n$ .

Dynamers are generally sensitive to the feed concentration of the starting materials, and this was next evaluated for the polymerization of compounds **1** and **2d**. In the concentration range of 0.125–2.5 M, all reactions resulted in polymer species with similar  $^1\text{H-NMR}$  spectra (Figure S92), and DOSY analysis revealed a clear inverse dependency between the diffusion coefficients and the feed concentration (Table S5, Figure S93–S100). However, the GPC analysis resulted in a more clear influence of the feed concentration (Figure 7b, Table S6, Figure S101–S108). The molecular weights of the polymers increased steadily in the concentration range from 0.125 M to 0.5 M of the starting materials, reaching a plateau between 0.5 M to 1.5 M. This behavior is consistent with an isodesmic polymerization mechanism,<sup>56</sup> as proposed for certain supramolecular polymers in which the interactions between the repeating units display equal association constants. However, at feed concentrations higher than 2.0 M, the molecular weights of the dynamers decreased to some extent, likely in response viscosity effects and slower polymerization.

The responsive behavior of the polymers was investigated by adding monofunctional compounds (**4**, **5**) or bifunctional compound **2b** as stimuli. The results indicate that the

dynamer underwent substantial changes in response to the added reagents. Thus, after exposure to the stimuli, the product solutions produced significantly higher diffusion coefficients than the original dynamer sample (**Figure 8a**, Table S7). Assuming that the viscosity of the solutions remains unchanged under these conditions, the results indicate that the polymer chains were shorter after responding to the stimuli.<sup>53</sup> At the same time, the changes observed in the <sup>1</sup>H-NMR spectra were relatively minor since the functional groups are similar before and after the reaction (Figure S109). However, as shown by GPC analysis (**Figure 8b**, Table S8), the molecular weight of the dynamer experienced significant drops after the stimuli exposures. The monofunctional compounds **4** and **5** induced changes that resulted in smaller polymer chains since they would act as polymerization stoppers. Compound **2b**, on the other hand, would favor macrocyclization over polymerization, which would also could break down the polymer. Even though no precipitate was observed by the naked eye in the reaction between compound **3d** and dinitroalkane **2b**, the peak in the GPC profile at around 30 min retention time (**Figure 8b**, red trace) is consistent with the GPC profile of lowellane **7** (Figure S59). These results all demonstrate the depolymerization of the dynamer induced by different stimuli.

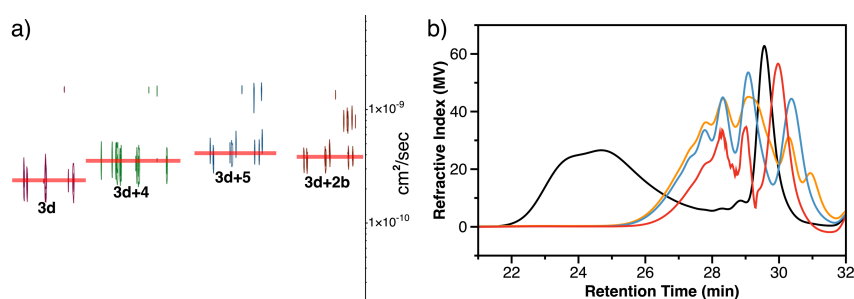


**Figure 8:** a) Pseudo-2D DOSY plots of dynamer **3d** before and after reaction with compounds **4**, **5**, or **2b**; b) GPC profiles of dynamer **3d** in the absence (black) or presence of compounds **4** (blue), **5** (orange), or **2b** (red).\*

## Conclusions

In summary, a series of dynamic covalent polymers have been synthesized through the nitroaldol reaction, leading to structures with linear and intriguing cyclic topologies. The use of dinitroalkanes efficiently resulted in dynamers with higher degrees of polymerization than corresponding structures based on nitromethane,<sup>3</sup> pronounced for building blocks with longer alkyl chains. A complex interplay between linear dynamers and macrocyclic oligomers were observed for shorter dinitroalkanes, where polymerization and depolymerization coupled with phase change of specific macrocycles occurred. This precipitation-driven macrocyclization represents the first dynamic systemic self-sorting process from a nitroaldol dynamer system. Furthermore, the adaptivity of the dynamers could be clearly shown, where the polymers responded to external stimuli through depolymerization and rearrangement of the polymer chains.

These results constitute important steps towards a detailed understanding of complex dynameric systems, and can lead to useful applications of nitroaldol-based dynamers where the controlled reversible nature is of importance. Such applications can be found in many areas, ranging from 3D-printing, surface adhesion, and degradable materials, to drug delivery, wound dressing, and matrices undergoing self-healing. We also expect that the unique features of the dynamic nitroaldol polymers will enable them to find use in a wide variety of neighboring fields, such as systems chemistry, porous self-assembled materials and frameworks, surface science, controlled adhesion technology, degradable and recyclable

materials for temporary utility, etc. Some of these uses have great potential to become more widespread applications, as they can lead to “smart”, programmable, adaptive-responsive materials.

## Acknowledgments

Y.Q. thanks the China Scholarship Council for a special scholarship award. We thank Wendy Gavin (UMass Lowell) for technical support. Mass spectral data were obtained at the University of Massachusetts Mass Spectrometry Core Facility, RRID:SCR\_019063. We thank Dr. Steve Eyles and Dr. Cedric Bobst (UMass Amherst) for their kind help on HRMS measurements.

## References

- (1) Durand-Silva, A.; Cortés-Guzmán, K. P.; Johnson, R. M.; Perera, S. D.; Diwakara, S. D.; Smaldone, R. A. *ACS Macro Lett.* **2021**, *10* (4), 486–491.
- (2) Zheng, N.; Xu, Y.; Zhao, Q.; Xie, T. *Chem. Rev.* **2021**, *121* (3), 1716–1745.
- (3) Karalius, A.; Zhang, Y.; Kravchenko, O.; Elofsson, U.; Szabó, Z.; Yan, M.; Ramström, O. *Angew. Chem. Int. Ed.* **2020**, *59* (9), 3434–3438.
- (4) Zhang, Y.; Qi, Y.; Ulrich, S.; Barboiu, M.; Ramström, O. *Mater. Chem. Front.* **2020**, *4* (2), 489–506.
- (5) Canal-Martín, A.; Pérez-Fernández, R. *ACS Omega* **2020**, *5* (41), 26307–26315.
- (6) Greenlee, A. J.; Wendell, C. I.; Cencer, M. M.; Laffoon, S. D.; Moore, J. S. *Trends Chem.* **2020**, *2* (12), 1043–1051.
- (7) Lijsebetten, F. V.; Holloway, J. O.; Winne, J. M.; Prez, F. E. D. *Chem. Soc. Rev.* **2020**, *49* (23), 8425–8438.
- (8) Morgan, F. L. C.; Moroni, L.; Baker, M. B. *Adv. Healthc. Mater.* **2020**, *9* (15), 1901798.
- (9) Marco-Dufort, B.; Iten, R.; Tibbitt, M. W. *J. Am. Chem. Soc.* **2020**, *142* (36), 15371–15385.
- (10) Su, D.; Coste, M.; Diaconu, A.; Barboiu, M.; Ulrich, S. *J. Mater. Chem. B* **2020**, *8* (41), 9385–9403.
- (11) Chakma, P.; Konkolewicz, D. *Angew. Chem. Int. Ed.* **2019**, *58* (29), 9682–9695.
- (12) Liu, Y.; Jia, Y.; Wu, Q.; Moore, J. S. *J. Am. Chem. Soc.* **2019**, *141* (43), 17075–17080.
- (13) Christensen, P. R.; Scheuermann, A. M.; Loeffler, K. E.; Helms, B. A. *Nat. Chem.* **2019**, *11* (5), 442–448.
- (14) Zhang, Y.; Zhang, Y.; Ramström, O. *Catal. Rev.* **2019**, 1–30.
- (15) Hartman, A. M.; Gierse, R. M.; Hirsch, A. K. H. *Eur. J. Org. Chem.* **2019**, *2019* (22), 3581–3590.
- (16) Orrillo, A. G.; Escalante, A. M.; Martinez-Amezaga, M.; Cabezudo, I.; Furlan, R. L. E. *Chem. Eur. J.* **2018**, *25* (5), 1118–1127.
- (17) Frei, P.; Hevey, R.; Ernst, B. *Chem. Eur. J.* **2018**, *25* (1), 60–73.
- (18) Winne, J. M.; Leibler, L.; Prez, F. E. D. *Polym. Chem.* **2019**, *10* (45), 6091–6108.
- (19) Liu, Y.; Lehn, J.-M.; Hirsch, A. K. H. *Acc. Chem. Res.* **2017**, *50* (2), 376–386.
- (20) Zhang, Y.; Barboiu, M. *Chem. Rev.* **2016**, *116* (3), 809–834.
- (21) Roy, N.; Bruchmann, B.; Lehn, J.-M. *Chem. Soc. Rev.* **2015**, *44* (11), 3786–3807.
- (22) Hirsch, A. K. H.; Buhler, E.; Lehn, J. *J. Am. Chem. Soc.* **2012**, *134* (9), 4177–4183.
- (23) Wojtecki, R. J.; Meador, M. A.; Rowan, S. J. *Nat. Mater.* **2011**, *10* (1), 14–27.
- (24) Lei, H.; Wang, S.; Liaw, D. J.; Cheng, Y.; Yang, X.; Tan, J.; Chen, X.; Gu, J.; Zhang, Y. *ACS Macro Lett.* **2019**, *8* (5), 582–587.
- (25) Wang, Y.; Xing, P.; An, W.; Ma, M.; Yang, M.; Luan, T.; Tang, R.; Wang, B.; Hao, A. *Langmuir* **2018**, *34* (45), 13725–13734.
- (26) Wen, Z.; McBride, M. K.; Zhang, X.; Han, X.; Martinez, A. M.; Shao, R.; Zhu, C.; Visvanathan, R.; Clark, N. A.; Wang, Y.; Yang, K.; Bowman, C. N. *Macromolecules* **2018**, *51* (15), 5812–5819.
- (27) Zhanan Zou, Y. L., Chengpu Zhu. *Sci. Adv.* **2018**, *4* (2), eaaq0508.
- (28) Mighani, H. *J. Polym. Res.* **2020**, *27* (6).



- (30) Chavez, A. D.; Evans, A. M.; Flanders, N. C.; Bisbey, R. P.; Vitaku, E.; Chen, L. X.; Dichtel, W. R. *Chem. Eur. J.* **2018**, *24* (16), 3989–3993.
- (31) Sims, M. B.; Patel, K. Y.; Bhatta, M.; Mukherjee, S.; Sumerlin, B. S. *Macromolecules* **2018**, *51* (2), 356–363.
- (32) Chao, A.; Negulescu, I.; Zhang, D. *Macromolecules* **2016**, *49* (17), 6277–6284.
- (33) Jiang, Y.; Hadjichristidis, N. *Angew. Chem. Int. Ed.* **2021**, *60* (1), 331–337.
- (34) Kumar Raut, S.; Kumar Behera, P.; Subhra Pal, T.; Mondal, P.; Naskar, K.; K. Singha, N. *Chem. Commun.* **2021**, *57* (9), 1149–1152.
- (35) Hou, I. C.-Y.; Hu, Y.; Narita, A.; Müllen, K. *Polym. J.* **2017**, *50* (1), 3–20.
- (36) Hufendiek, A.; Lingier, S.; Du Prez, F. E. *Polym. Chem.* **2019**, *10* (1), 9–33.
- (37) Robinson, L. L.; Self, J. L.; Fusi, A. D.; Bates, M. W.; Read de Alaniz, J.; Hawker, C. J.; Bates, C. M.; Sample, C. S. *ACS Macro Lett.* **2021**, *10* (7), 857–863.
- (38) Tajbakhsh, S.; Hajiali, F.; Marić, M. *ACS Applied Polymer Materials* **2021**, *3* (7), 3402–3415.
- (39) Prasanna Kar, G.; Osman Saed, M.; Michael Terentjev, E. *J. Mater. Chem. A* **2020**, *8* (45), 24137–24147.
- (40) Liu, T.; Zhao, B.; Zhang, J. *Polymer* **2020**, *194*, 122392.
- (41) Li, S.; Zuo, C.; Zhang, Y.; Wang, J.; Gan, H.; Li, S.; Yu, L.; Zhou, B.; Xue, Z. *Polym. Chem.* **2020**, *11* (36), 5893–5902.
- (42) Zhang, X.; Wang, S.; Jiang, Z.; Li, Y.; Jing, X. *J. Am. Chem. Soc.* **2020**, *142* (52), 21852–21860.
- (43) Bednarek, M.; Kubisa, P. *Polym. Chem.* **2019**, *10* (15), 1848–1872.
- (44) Azcune, I.; Odriozola, I. *Eur. Polym. J.* **2016**, *84*, 147–160.
- (45) Vongvilai, P.; Angelin, M.; Larsson, R.; Ramström, O. *Angew. Chem. Int. Ed.* **2007**, *46* (6), 948–950.
- (46) Luzzio, F. A. *Tetrahedron* **2001**, *57* (6), 915–945.
- (47) Ballini, R.; Bosica, G. *J. Org. Chem.* **1997**, *62* (2), 425–427.
- (48) Henry, L. *Comptes rendus hebdomadaires des séances de l'Académie des sciences* **1895**, *120*, 1265–1268.
- (49) Angelin, M.; Vongvilai, P.; Fischer, A.; Ramström, O. *Eur J Org Chem* **2010**, *2010* (33), 6315–6318.
- (50) Vongvilai, P.; Larsson, R.; Ramström, O. *Adv. Synth. Catal.* **2008**, *350* (3), 448–452.
- (51) Angelin, M.; Vongvilai, P.; Fischer, A.; Ramström, O. *Chem. Commun.* **2008**, No. 6, 768–770.
- (52) Schulz, M.; Wimmer, K.; Görls, H.; Westerhausen, M. *Z. Naturforsch. B* **2011**, *66* (6), 611–623.
- (53) Groves, P. *Polym. Chem.* **2017**, *8* (44), 6700–6708.
- (54) Sisco, S. W.; Larson, B. M.; Moore, J. S. *Macromolecules* **2014**, *47* (12), 3829–3836.
- (55) Zhang, W.; Moore, J. S. *J. Am. Chem. Soc.* **2005**, *127* (33), 11863–11870.
- (56) De Greef, T. F. A.; Smulders, M. M. J.; Wolffs, M.; Schenning, A. P. H. J.; Sijbesma, R. P.; Meijer, E. W. *Chem. Rev.* **2009**, *109* (11), 5687–5754.
- (57) Hodge, P. *React. Funct. Polym.* **2014**, *80*, 21–32.
- (58) Stille, J. K. *J. Chem. Educ.* **1981**, *58* (11), 862.